DNA Gold Nanoparticle Nanocomposite Films for Chemiresistive Vapor Sensing

ARTICLE *in* LANGMUIR · OCTOBER 2013

Impact Factor: 4.46 · DOI: 10.1021/la402626p · Source: PubMed

5 AUTHORS, INCLUDING:

Kan Fu
University of Connecticut
6 PUBLICATIONS **13** CITATIONS
SEE PROFILE

Shihui Li
Pennsylvania State University
13 PUBLICATIONS **68** CITATIONS
SEE PROFILE

Xiaoqiang Jiang
University of Connecticut
10 PUBLICATIONS **72** CITATIONS
SEE PROFILE

Yong Wang
Nanjing University of Posts and Telecommuni…
703 PUBLICATIONS **14,900** CITATIONS
SEE PROFILE

Langmuir

Article

pubs.acs.org/Langmuir

DNA Gold Nanoparticle Nanocomposite Films for Chemiresistive Vapor Sensing

Kan Fu,[†] Shihui Li,[§] Xiaoqiang Jiang,[‡] Yong Wang,[§] and Brian G. Willis*[,‡]

[†]Department of Materials Science and Engineering, University of Connecticut, Storrs, Connecticut 06269, United States
[‡]Department of Chemical and Biomolecular Engineering, University of Connecticut, Storrs, Connecticut 06269, United States
[§]Department of Bioengineering, Pennsylvania State University, University Park, Pennsylvania 16802, United States

ABSTRACT: Chemiresistive vapor sensors combining functionalized gold nanoparticles and single-stranded DNA oligomers are investigated to enhance specificity in chemical sensing. Sensors are made by depositing DNA-functionalized gold nanoparticles onto microfabricated electrodes using four distinct sequences. Sensor performance is evaluated for response to relative humidity and exposure to vapor analytes including ethanol, methanol, hexane, dimethyl methylphosphonate, and toluene under different relative humidity. It is found that sensors display a nonmonotonic resistance change toward increasing humidity due to the combined effects of hydration induced swelling and ionic conduction. Responses to vapor analytes show sequence-dependent patterns as well as a strong influence of humidity. Overall, the findings are encouraging for using DNA oligomers to enhance specificity in chemical sensing.

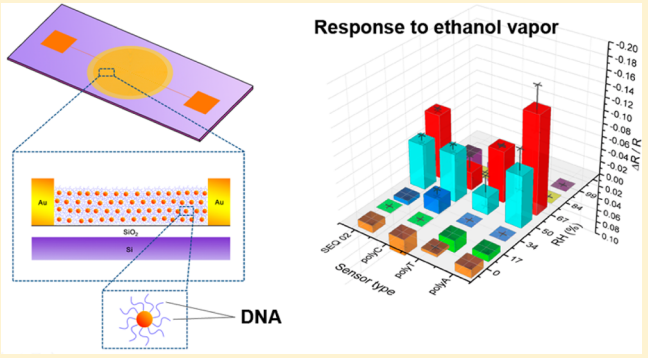

INTRODUCTION

Chemiresistive sensing of vapors using chemically functionalized gold nanoparticle (AuNP) films has been intensively investigated in recent years. The level of interest is based on several favorable characteristics including response speed, sensitivity, reversibility, potential for miniaturization, and ease of integration with microelectronics.[1−4] Typically, an electric current through a nanoparticle film is measured under steady ac or dc voltage bias, and the current response is sensitive to the sorption of vapors, which may yield a sensitive probe of the vapor composition. The simplicity of chemiresistor designs provides practical benefits compared to other devices that use more complex transduction mechanisms such as chemitransistors,[5,6] fluorescence-based detectors,[7] surface acoustic wave (SAW) sensors,[8] fiber-optic vapor sensors,[9] and surface-enhanced Raman scattering (SERS) sensors.[10]

One of the most attractive aspects of AuNPs as chemiresistor elements is their high flexibility toward surface modification with thiol-functionalized organic molecules, enabling a large library of monolayer-protected gold metal clusters (Au-MPCs). Partitioning of volatile organic compounds into the organic capping layers[2,3] leads to a series of effects, including changes in electron hopping distance, alteration of dielectric constants, and possible activation of mobile charged species.[2] Because of differences of sorption parameters for different analytes, variations in electrical responses are observed. In this way, vapors have been identified by principal component analysis of data from arrays of Au-MPC sensors with different functionalities.[3,11] These arrays are sometimes referred to as "electronic noses" because they mimic mammalian olfaction.

A limitation of current Au-MPCs is the general difficulty with achieving specificity of sensor response characteristics. Specificity is limited by the range of solubility characteristics that can be achieved with organic capping layers. A new direction that may enable enhanced specificity is to incorporate nucleic acid oligomers as molecular recognition elements. The interest in nucleic acid oligomers is partly motivated by the immense number of base sequences that can be created. The number of possible unique receptor configurations scales with the length N of the oligomer as 4^N, giving rise to a large diversity of sensing elements. In addition, DNA oligomers may be used to develop aptamers, which are short oligonucleotides that bind target analytes with high specificity. For example, aptamers have been developed for small molecule targets including cocaine, ATP,[12] and trinitrotoluene (TNT).[13]

Though oligomeric nucleotide sequences are most commonly used in solution, recent reports have included fluorescence-based solid-state sensors that respond to target vapor analytes through sorption-induced changes of fluorescence intensity.[10] White et al. used 29 different single-stranded (ss) DNA sequences tagged with dye molecules to create sensor arrays and measured their response to volatile compounds. The number of distinct sequences employed was roughly twice as many as other MPC-based sensor arrays reported to date.[14] Others have proposed modifying nucleobases with fluorescent groups to give fluorescence

Received: July 11, 2013
Revised: September 19, 2013
Published: October 10, 2013

responses to organic vapors.[15] Polynucleotides have also been used to functionalize chemitransistors made from carbon nanotubes (CNT)[16,17] and graphene[18] as well as nanofunctionalized organic field-effect transistors.[19] These studies demonstrate the potential for sequence-dependent chemical recognition capability with DNA oligomers.

A significant challenge for DNA-based vapor sensing is to extend their function from solution-based to solid-state devices. Water interacts strongly with DNA, altering the microscopic structures of both double-stranded[20,21] and single-stranded DNA[21] molecules so that sensitivity to water may be expected in solid-state devices. Many prior studies of chemiresistor devices have used relatively hydrophobic sensing materials that are not particularly sensitive to humidity,[22,23] but there are at least a few examples where sensitivity to water vapor has been observed.[24] Control of humidity effects in solid-state DNA-based sensing has been considered in some studies,[14,17] but the effect of water on chemiresistive vapor sensing has not been systematically studied. As DNA is a highly polar molecule with ionized phosphate groups and multiple hydration shells,[25,26] it is anticipated that humidity may have a significant effect on DNA-based absorptive sensors. It is therefore imperative to measure the effects of humidity on such materials.

In this work, we investigate the use of DNA oligomers as surface layers on AuNPs for chemiresistive vapor sensing. We show that a film of oligonucleotide-functionalized AuNPs can be produced through an aqueous-based thiol−gold conjugation process followed by drop-casting onto microfabricated electrodes. The films share similar macroscopic morphology with MPC films prepared from thiolated organic capping layers but exhibit distinctive electrical properties. As anticipated, the sensors show a significant response to water vapor, but unlike the monotonic responses seen in most vapor sensors, the response is dichotomous. This behavior is explained in the context of film nanostructure and polyelectrolyte conduction mechanisms. Using four different ss-DNA sequences, sensitivities to organic vapors are studied under carefully controlled humidity levels. Maximum response sensitivity is observed for intermediate humidity levels, and sequence-dependent responses are observed. This study demonstrates that oligonucleotide-functionalized AuNPs are useful new materials for chemiresistive vapor sensing.

EXPERIMENTAL METHODS

Preparation of Oligonucleotide-Functionalized AuNPs. Citrate-stabilized AuNPs (10 nm diameter, OD1), tris(2-carboxyethyl)-phosphine hydrochloride (TCEP), glacial acetic acid, sodium acetate, sodium chloride (NaCl), 1-octanethiol, and 8-mercapto-1-octanol were purchased from Sigma-Aldrich (St. Louis, MO). Tris base was purchased from Fisher Scientific (Suwanee, GA). All aqueous solutions were made with double-distilled water (dd-H_2O). Single-stranded oligonucleotide sequences were purchased from Integrated DNA Technologies Inc. (Coralville, IA).

SEQ 02, poly A, poly T, and poly C were used to functionalize citrate-stabilized AuNPs following a previously reported protocol with minor modifications.[27] To activate the thiol-modified DNA sequences, 3 μL of DNA solution (1 mM), 1 μL of acetate buffer (500 mM, pH 5.2), and 1.5 μL of TCEP (10 mM) were mixed with H_2O to obtain a final volume of 10 μL and incubated for 1 h at room temperature. The mixture was added to 1 mL of as-received citrate-stabilized AuNP solution and reacted for 16 h in the dark at room temperature. Subsequently, 10 μL of Tris acetate (500 mM, pH 8.2) buffer was added into the AuNP solution, followed by the addition of 110 μL of NaCl (1.0 M) dropwise with gentle shaking. The whole mixture was incubated in the dark for another 24 h before use. In control experiments, H_2O was added to 1 mL of AuNP solution in place of DNA, prior to the 16 h incubation step.

Table 1. DNA Oligomers

name	sequence (5′ to 3′)
SEQ 01	/Cy-5[a]/AAA AAA AAA GAG GAG GAA AAG GAG T
SEQ 02	/ThioMC6-D[b]/TTT TTA CTC CTT TTC CTC CTC TTT T
Poly A	/ThioMC6-D[b]/AAA AAA AAA AAA AAA AAA AAA A
Poly T	/ThioMC6-D[b]/TTT TTT TTT TTT TTT TTT TTT T
Poly C	/ThioMC6-D[b]/CCC CCC CCC CCC CCC CCC CCC C

[a]Cyanine fluorescence group. [b]Thiol functionalization group $-C_6H_{12}-SH$.

Fabrication of DNA-AuNP Chemiresistors. Circular interdigitated gold electrodes (20 μm width, 20 μm spacing, and 200 nm thick) were fabricated on 4 in. silicon wafers by standard photolithography and e-beam evaporation techniques. Each device chip was 40 mm^2 in size and had a single chemiresistor with an area of 7 mm^2. The total electrode perimeter is estimated as 290 mm. Substrates were cleaned with oxygen plasma for 5 min prior to drop-casting gold nanoparticle solutions. To remove most of the buffer salts (e.g., NaCl) from DNA-functionalized gold nanoparticle storage solutions, 1 mL of nanoparticle solution was subjected to centrifugation at relative centrifugation force (RCF) = 15000g for 40 min, the supernatant was removed, and the concentrate was redispersed in 1.5 mL of dd-H_2O. This washing procedure was repeated twice. The final product obtained from centrifugation was suspended in 20 μL of dd-H_2O to form a DNA-functionalized gold nanoparticle concentrate. The concentrate for drop-casting was standardized using a UV−vis spectrophotometer (Thermo Scientific NanoDrop ND-1000) to have absorbance = 2.5. For drop-casting, 4 μL of gold nanoparticle concentrate was deposited on each sensor area. The droplet readily wets the electrode areas and was evaporated under a dry air atmosphere at room temperature. The dc resistances measured in air have a resistivity in the range of 300−800 kΩ.

Characterization of DNA-AuNP Films and Sensor Electrodes. DNA-functionalized AuNPs were characterized both in solution and in dried drop-cast forms. In solution, SEQ 02-modified AuNPs were studied with the aid of a fluorescence-based method.[28] After preparation of SEQ 02-modified AuNPs, 100 μL of AuNP solution was washed with dd-H_2O twice by centrifugation at 15000g for 40 min to remove free SEQ 02 DNA. The pellet of AuNPs was subsequently dispersed into a 100 μL NaCl solution (100 mM). The concentration of AuNP solution was determined by measuring the absorbance at 520 nm using a UV−vis spectrophotometer (Thermo Scientific NanoDrop ND-1000). Afterward, 1.5 μL of Cy5-labeled SEQ 01 (100 μM) was added to the AuNP solution to hybridize with the SEQ 02 immobilized on the AuNPs. The mixture was kept in the dark with gentle shaking at room temperature for 2 h. Two additional rounds of washing with 100 mM NaCl solution were carried out, and the unhybridized SEQ 01 in the supernatant was measured after each washing step. The concentration of free SEQ 01 was determined using a fluorospectrometer (Thermo Scientific NanoDrop ND-3300). The quantity of SEQ 02 chemisorbed on AuNPs approximately equals the amount of SEQ 01 consumed through complementary base paring. The amount of SEQ 01 consumed due to hybridization was determined as the difference between the initial amount of SEQ 01 added and free, unhybridized SEQ 01 measured in the supernatant, summed from each of the three washings.

$$\text{DNA per AuNP} = \frac{\text{mol}_{\text{initial amount of SEQ 01}} - \text{mol}_{\text{unhybridized SEQ 01}}}{\text{mol}_{\text{AuNP}}}$$

Surface characterization of dried DNA-functionalized gold nanoparticle films was also performed using X-ray photoelectron spectroscopy (XPS) (Kratos AXIS 165) with a monochromatic Al Kα X-ray source. Gold nanoparticle concentrates after centrifugation and washing were drop-cast on oxygen-plasma treated indium foils before insertion in to the XPS vacuum chamber. Surface analysis was

dx.doi.org/10.1021/la402626p | Langmuir 2013, 29, 14335−14343

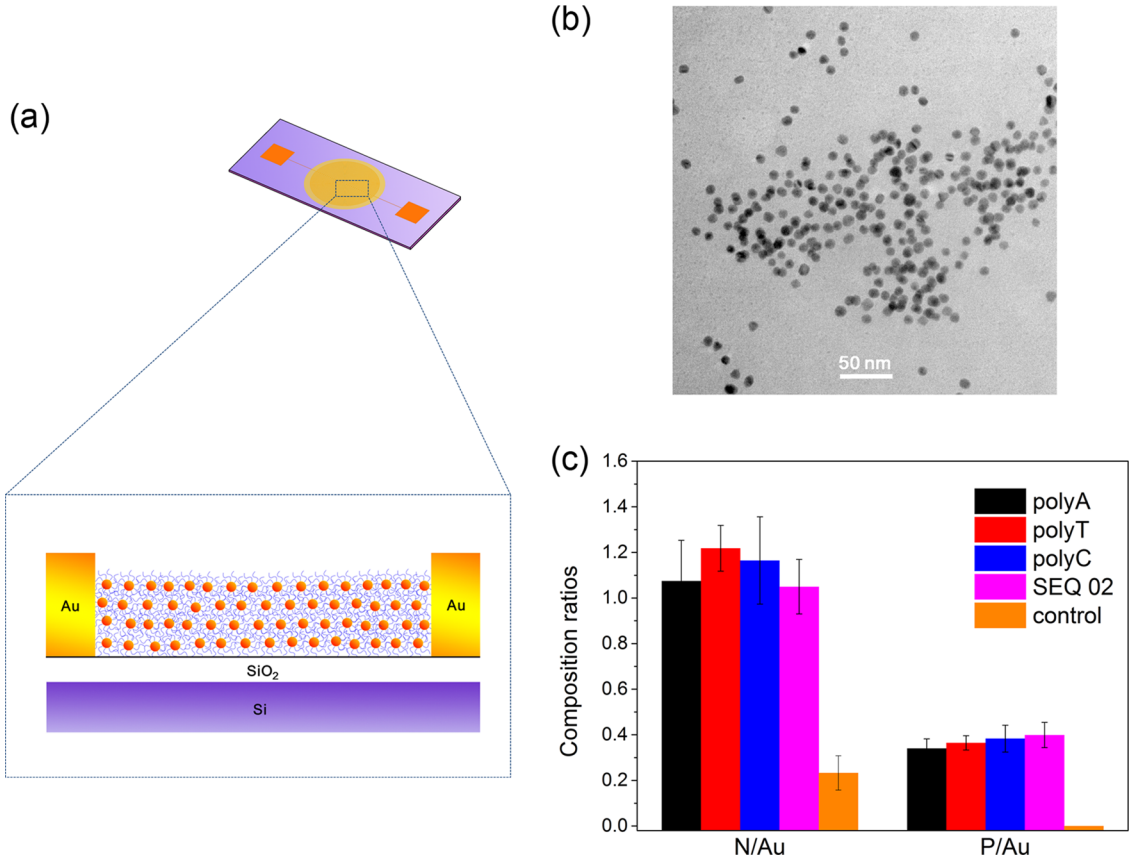

Figure 1. (a) Sensor schematic of a drop-cast film of DNA-functionalized AuNPs covering microfabricated electrodes. AuNPs bridge the gaps between gold electrodes (not drawn to scale). (b) TEM image of 10 nm DNA-functionalized AuNPs. (c) Surface composition of nitrogen and phosphorus on DNA-functionalized AuNPs compared to controls with citrate-capped AuNPs; control samples have no P signal.

performed on both DNA-functionalized AuNPs and control nanoparticles without DNA to measure elemental composition. The DNA coverage obtained from SEQ 02 characterization was used as a reference for estimating poly A, poly T, and poly C coverage with XPS. This was done by comparison of the N and P elemental percentages with SEQ 02 as a reference. Electrochemical impedance spectroscopy (EIS) measurements were performed using an electrochemical workstation (CH Instruments 660D) under a two-electrode setting with a testing range of 0.1 Hz to 100 kHz.

Vapor Sensing. For sensing experiments, sensor devices were wire-bonded (West Bond 747630E) to a two-lead chip carrier. The two terminals of each chip carrier were connected to a source measurement unit (Keithley 2612). The chip carrier was fitted onto a custom built 0.5 cm × 2 cm × 15 cm flow cell fabricated from aluminum and sealed with O-rings. The flow cell allows concurrent testing of up to eight devices, with an effective chamber volume for each sensor of approximately 2 cm^3. The source measurement unit was programmed to generate a 1.0 V_{p-p} square wave at 500 Hz, and dc current was recorded in the middle of each positive half-cycle. Data collection was performed using TSP Script software provided with the source measurement unit. Ultrahigh-purity nitrogen (Air Gas, purity of 99.999%) was used as a diluent and carrier gas. Saturated water and organic vapors were generated using bubblers. For studies of the effect of humidity on sensor response, seven relative humidity (RH) levels were investigated: 0%, 17%, 34%, 50%, 67%, 84%, and 100%, with a total flow rate of 600 sccm. The effect of RH on sensor response to organic vapors was measured at 0%, 17%, 34%, 50%, 67%, 84%, and 99%. Because of the inclusion of additional gas streams, the total flow rate was 620 sccm. Organic vapor levels are quantified as the ratio of the vapor partial pressure to its saturation vapor pressure (p/p_0) at 22 °C. For measuring the device response to organic vapors, special care was taken to maintain a constant water mole fraction in the gas phase. This was necessary to avoid sensor responses from changes in the humidity of the input flow streams. In all vapor sensing experiments, a steady baseline was achieved before adding organic vapors. After each experiment, the sensors were purged by humidified nitrogen of the specified RH for 5 min followed by dry nitrogen for 5 min. The sensors were then stored in dark containers filled with N_2 to minimize light-induced and oxidative DNA damage. All experiments were carried out at an ambient temperature of 22 ± 1 °C.

RESULTS AND DISCUSSION

Characterization of DNA-AuNP Surface Functionalization. The attachment of thiol-functionalized DNA to AuNPs was apparent from visual inspection. For all sequences studied, DNA-functionalized AuNPs were observed to maintain good dispersion in solution. By contrast, addition of buffer solution to citrate-stabilized AuNPs without DNA resulted in nanoparticle aggregation within a few hours. A change in solution color from light red to light purple was an indication of aggregation. These observations are consistent with superior stabilization of nanoparticles in electrolyte solutions through synergistic electrostatic and steric mechanisms.[29] AuNPs with citrate capping alone are known to be less resistant to aggregation as they are predominantly electrostatically stabilized.[30] For SEQ 02, the fluorescence-based technique shows that surface coverage is 40 (±6) DNA oligonucleotides per nanoparticle. For 10 nm diameter particles, the surface density is 1.3 × $10^{13}/cm^2$, which can be compared with literature data: 5 × $10^{12}/cm^2$ [31] and 3.7 × $10^{13}/cm^2$ [32,33] for 25-mers and 1.4 × $10^{13}/cm^2$ for a 15-mer.[34] Previous studies have shown that ss-DNA oligomers of 25-mer size are generally

dx.doi.org/10.1021/la402626p | Langmuir 2013, 29, 14335−14343

coiled structures that extend 0.7 to 1.0 nm from the particle surface.[35−37]

Surface analysis was performed with XPS to verify that DNA is present on gold nanoparticle films after drop-casting and drying. Figure 1a shows measurements of nitrogen and phosphorus content for DNA-functionalized AuNPs compared with control samples. N/Au atomic ratios of all DNA-functionalized samples were within the range of 1.0−1.2, and P/Au atomic ratios were approximately 0.3. Because of the minute amount of sulfur per molecule, no sulfur 2p signals were observed on any sample.[32] The phosphorus signal from the DNA-functionalized AuNP films serves as direct evidence of successful DNA adsorption onto nanoparticles. No phosphorus is measured on control samples. There is a small N 1s signal from control samples that may originate from residual buffer salts, but the DNA samples have a 3× higher N 1s signal that is consistent with DNA coverage of the AuNPs. Estimates of surface coverage for poly A-, poly T-, and poly C-functionalized AuNPs are obtained by comparing XPS surface phosphorus percentages to SEQ 02 as a reference. Results are 42, 36, and 36 molecules/particle for poly A, poly T, and poly C, respectively. Other elemental signatures such as C and O were not useful for distinguishing DNA and control samples.

Electrical Properties and Sensitivity to Relative Humidity. DNA-functionalized gold nanoparticle sensors display a distinctive dichotomous behavior in response to RH. In this study, R/R_0 is used to characterize the ratio of resistance at a specific RH to the resistance at RH = 0%, and $\Delta R/R$ is used to characterize sensor response to analytes at fixed RH. Water vapor is not treated as an analyte, but as an environmental factor that modifies the baseline resistance of the sensor at a specific RH. R_0 is the sensor baseline resistance at zero RH or in a dry atmosphere. For all sensors, R/R_0 increases from 1 at RH = 0% to around 2 at 34% and then decreases rapidly, reaching 0.01 above RH = 50% (Figure 2a). This dichotomous behavior is atypical for nanoparticle-based chemiresistive sensors. This can be seen by comparing water vapor sensing behavior between DNA-functionalized AuNPs and alkanethiol-functionalized AuNPs. To that end, 1-octanethiol- and 8-mercapto-1-octanol-functionalized AuNP sensors were prepared using the standard protocol by Woltjen et al.[1] and subjected to identical vapor testing conditions. The R/R_0 trends with increasing RH for these devices are shown in Figure 2b. The monotonic trends are similar to previously published AuNP chemiresitive sensors with alkanethiol-type ligands.[1,38] Similarly, studies of pure DNA films also report monotonous resistivity trends across the RH range from 0% to 100%.[39] The distinctive behavior of DNA-AuNP films is therefore an indication that the conduction mechanism of DNA-AuNP films has contributions from both nanoparticles and the polyelectrolyte matrix.

The distinctive response of DNA AuNP devices can be understood from two separate conduction mechanisms. At low RH levels (0%−40%), the upward trend in R/R_0 is governed predominantly by matrix-swelling effects common to AuNP chemiresistive sensors. In this RH range, the effects of ionic conduction are insignificant compared to the electronic current. At higher RH levels (40%−100%), ionic conduction becomes significant and R/R_0 decreases. Similar effects of decreasing resistivity at higher vapor concentrations have been observed in studies of tetraoctylammonium bromide (TOAB)-functionalized AuNPs.[2,40] In that study, residual ionic species solvated by vapors were proposed as one possible source of increasing

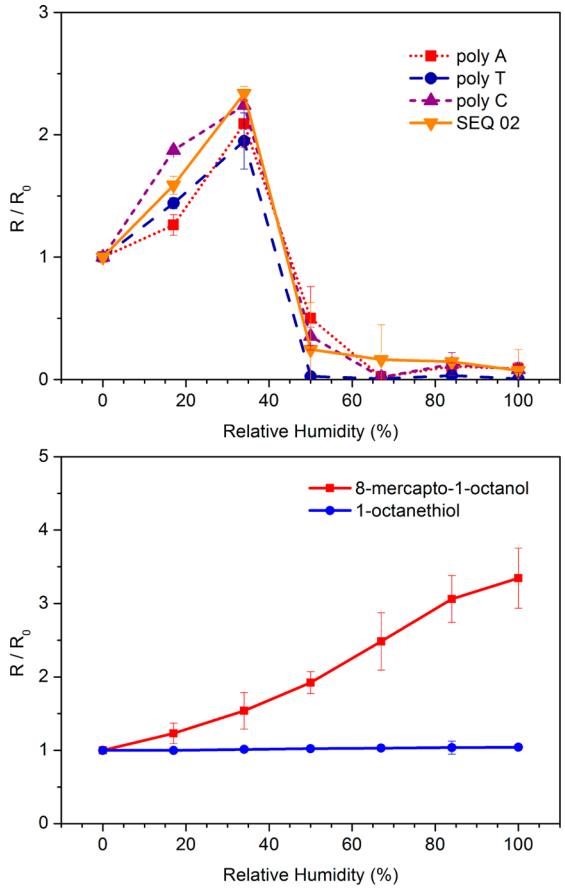

Figure 2. (a) Effect of RH on baseline resistance of DNA-functionalized AuNP films. (b) Effect of RH on resistance of two types of alkanethiol-functionalized AuNP films.

conductance. The difference here is that DNA intrinsically contains ionic species that may contribute to conductivity at high RH levels. Voids in the film may also contribute to ionic conduction, as water condensation on the hydrophilic SiO_2 surface under high RH levels is likely.[41]

The significant response to increasing humidity for all ss-DNA devices studied is indicative of the favorable hydration of DNA oligomers. Water is integral to DNA structure with significant interactions at both phosphate and base sites, and the hydration shell has been described as a monolayer of water on the DNA surface area.[42] Estimates for hydrated ds-DNA are near 30 H_2O per nucleotide pair with waters strongly bound even at 0% RH.[26] Base-specific interactions have been observed in crystallographic studies, but these effects are complicated by structure.[43] For example, it was reported that the strength of water interaction first decreases but then increases with increasing AT content.[42] In Figure 2a and other data, SEQ 02 has the strongest response to water even though it has significant T content and poly T has the weakest response. Further study is needed to separate base composition from sequence and structure effects.

To further characterize the conduction mechanisms, electrochemical impedance spectroscopy (EIS) measurements were performed. The EIS results are consistent with a RH-dependent conduction mechanism (Figure 3). At low RH levels, only a single semicircle is observed on the Nyquist plot, indicating an electron-transfer-limited process.[44] At higher RH levels of 50% for poly A, a linear response appears in the low-frequency

dx.doi.org/10.1021/la402626p | Langmuir 2013, 29, 14335−14343

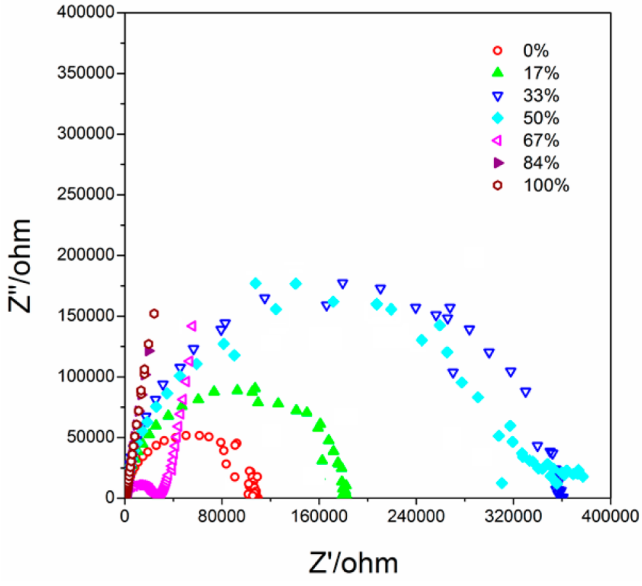

Figure 3. Nyquist plots recorded for poly A RH levels 0–100%.

region, which is characteristic of a diffusion-limited charge transfer process. The source of this diffusion-limited charge transfer is a frequency-dependent ion diffusion/transport in the polyelectrolyte (DNA).[44] As RH increases, the semicircle radius first increases and then decreases—a trend that corresponds closely with the dc resistance measured using the source measurement unit. In the range of RH from 84% to 100%, the linear portion of the curve becomes increasingly vertical, indicating increasing capacitive behavior, which confirms the dominance of ionic conduction.[45] These Nyquist plots substantially reflect the transition from electronic to ionic conduction as RH increases.

Vapor Sensing. Responses to several organic vapors were measured at constant RH for a range of different RH conditions. Figure 4a shows the response of four different DNA-AuNP sensors to hexane at RH = 0%. Sensor responses are expressed as the commonly used $\Delta R/R$, where R is the baseline resistance of the sensor at a given RH and ΔR is the vapor induced change from the baseline. The plots show a rapid response, good reversibility, and near-linear dependence on hexane vapor pressure. All four sequences show a response to hexane vapor, but there are clear sequence-dependent intensity differences. SEQ 02 and poly C have the largest response, while poly T has the smallest. Figure 4b shows the real-time sensor response of SEQ 02 to ethanol at different RH levels. Both positive and negative responses are observed, depending on RH, with a trend toward negative $\Delta R/R$ response at increasing RH. The SEQ 02 data show no significant response for the two highest RH values.

Combination plots of sensor responses to all organic vapors at different RH levels are shown in Figure 5. $\Delta R/R$ values are all positive (downward in the figure) when water vapor is not present, indicating a swelling dominated behavior. These positive responses are similar to that of water vapor (Figure 2a). However, mostly negative $\Delta R/R$ responses are observed for RH in the range of 50%–67%, while reduced responses are observed in the ranges of RH = 17%–34% and 84%–100%. The response patterns are sensitive to RH with highest sensitivity in the range of 50%–67%. Interestingly, this region is near where the sensitivity to water vapor peaks and then rapidly

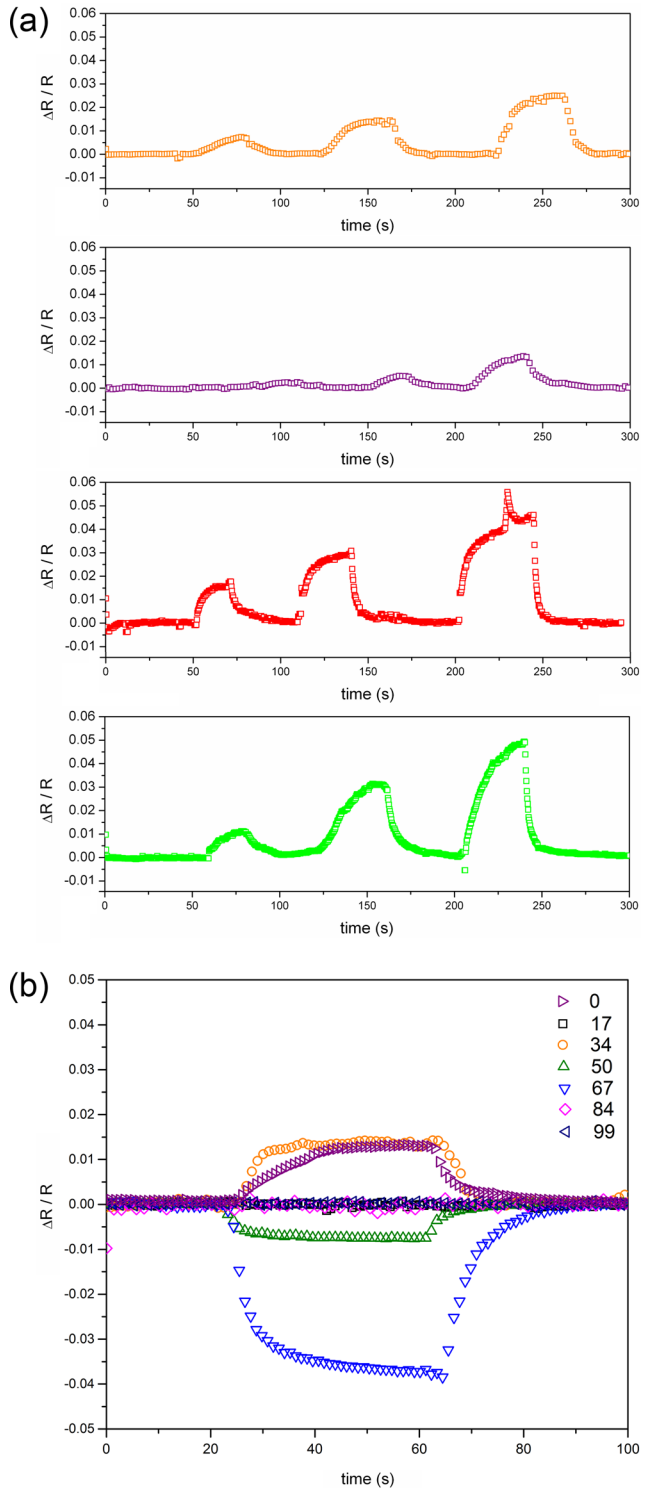

Figure 4. (a) Real-time response of four types of DNA-functionalized gold nanoparticle sensors on hexane vapor at RH = 0% with p/p_0 = 0.012, 0.024, and 0.036. From top to bottom: polyA, polyT, polyC, SEQ 02. (b) Real-time response of a SEQ 02 sensor against ethanol vapor equivalent to p/p_0 = 0.036 at seven RH levels ranging from 0% to 99%.

decreases, although the correlation is not simple. Qualitatively, the response patterns are similar for each of the different DNA sequences with sensitivities that peak in the same regions, but there are sequence-dependent patterns that distinguish each different DNA oligomer at a given RH as well as different

dx.doi.org/10.1021/la402626p | Langmuir 2013, 29, 14335–14343

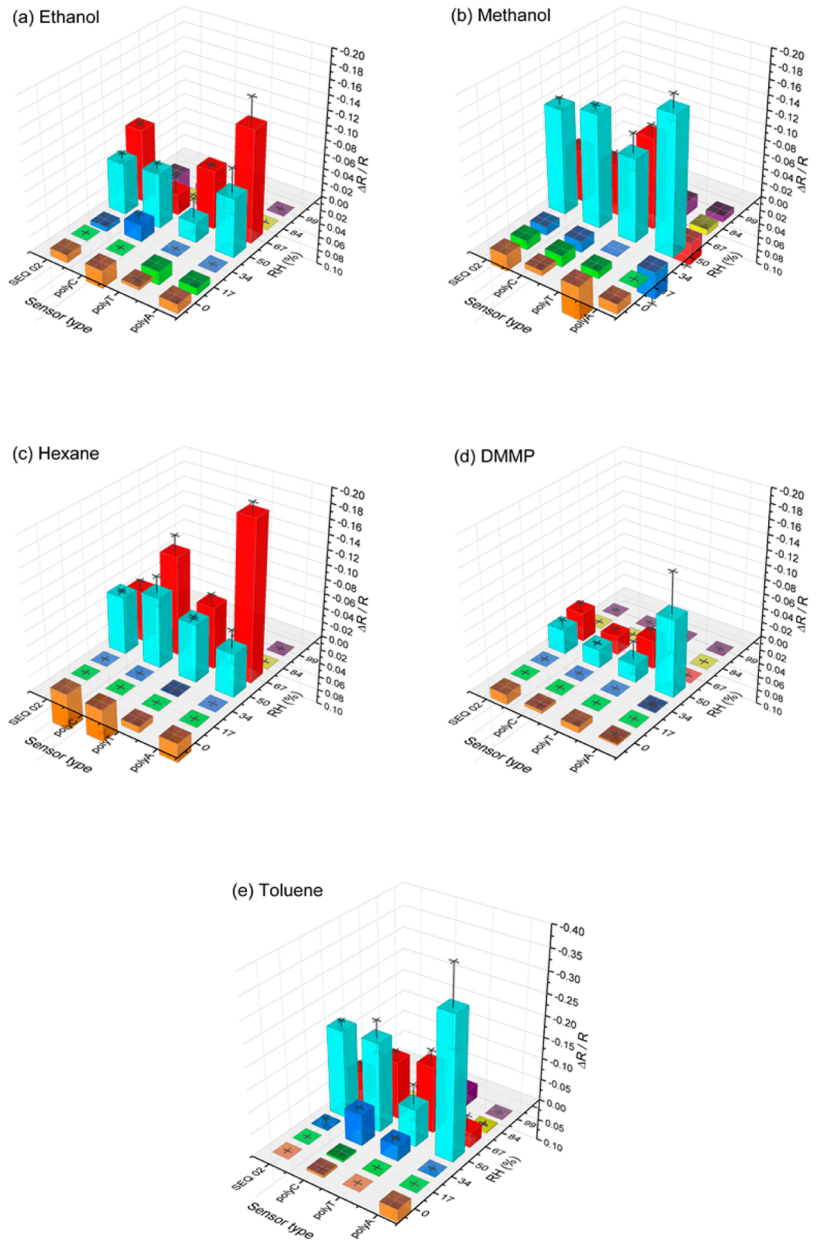

Figure 5. 3D bar charts of sensor response to five vapors across all RH levels (0%−99%) for (a) ethanol, (b) methanol, (c) hexane, (d) DMMP, and (e) toluene. Concentrations are p/p_0 = 0.036 for all five vapors.[47]

patterns with RH. For example, poly A has the strongest peak response to all vapors, but the RH dependence is different for each vapor. Absolute values of response signals vary between different devices, but the qualitative trends are reproducible.

Sensors fabricated with this method typically have a root-mean-square (rms) baseline noise on the order of 0.2%−0.3% that is not strongly dependent on humidity. Table 2 summarizes the sensitivity for the four types of sensors at two working conditions with RH levels of zero and 50%. Table 3 compares limits of detection (LOD) for ss-DNA with organothiol AuNP sensors that have been widely studied in the literature. For direct comparison, vapor concentrations have been converted to parts per million. Depending on the analyte, reported LOD values range from a few to a few hundred ppm.[46] LOD are dependent on signal-to-noise properties of the measurements, which are not commonly reported. Qualitatively, LOD of ss-DNA AuNP sensors are comparable to organothiol AuNP sensors. Both the response magnitudes and analyte trends are consistent with the prior studies using hexanethiol capping layers. Both sensors show similar responses for ethanol and higher sensitivity for toluene. Intermediate RH levels appear to improve the LOD values for the DNA-based sensors. The data for octanethiol have an order of magnitude lower LOD due to a much lower signal-to-noise level assumed in the calculation, but the qualitative trends for ethanol and toluene sensing are similar.

In field applications, cross-sensitivity to water is a complicating issue for sensors that function by vapor absorption into a condensed phase. Previous studies with SAW sensors have investigated the effects RH has on baseline and sensitivity toward organic vapors.[24] Similar effects are observed here in DNA-functionalized AuNP chemiresistive sensors, but the volcano-shaped response is distinctive from previous studies with alkanethiol AuNPs that generally report

dx.doi.org/10.1021/la402626p | *Langmuir* 2013, 29, 14335−14343

Table 2. Sensitivity of Four Types of DNA-AuNP Sensors to Five Vapors at Two RH Levels

		sensitivity[a]			
RH (%)	vapor	poly A	poly T	poly C	SEQ 02
0	ethanol	0.35	0.11	0.92	0.31
	methanol	0.14	0.44	0.20	0.75
	hexane	0.69	0.23	1.22	1.37
	DMMP	0.00	0.23	0.12	0.38
	toluene	0.82	0.19	0.35	0.23
50	ethanol	−2.17	−0.72	−1.06	−1.91
	methanol	−9.45	−3.09	−7.85	−7.64
	hexane	−1.59	−2.13	−4.50	−3.50
	DMMP	−2.83	−0.64	−0.66	−0.90
	toluene	−9.03	−2.36	−5.64	−5.58

[a]Slope from linear approximation of $\Delta R/R-p/p_0$ plots, in the form of Figure 6.

Table 3. Comparison of LODs of DNA-AuNP Sensors with Reported Alkanethiol Au Nanoparticle Sensors

	LOD (ppm)			
vapor	DNA (RH = 0%)[a]	DNA (RH = 50%)[a]	octanethiol[48,49]	hexanethiol[2]
ethanol	475	266	4.9−49	242
methanol	171	145	150	326
toluene	211	32	0.082−2.3	48

[a]Defined as three times the baseline noise divided by sensitivity as appeared in Table 2.

weakening sensor response with increasing RH.[40] We rationalize this behavior based on hydration and chain flexibility and their influence on the conduction mechanism. In a dry state, the sensor response is primarily from swelling of the composite organic−AuNP matrix, similar to alkanethiols, and we do not expect significant conformational changes in DNA upon adsorption of organic vapors. The weak response sensitivity for the range of RH levels from 17% to 34% is unexpected since it is weaker than both the dry state and intermediate humidity. It may be that at low RH water is held so tightly by the DNA so as to exclude organic sorption. The water may alter the DNA matrix to be more hydrophilic resulting in weaker interactions with hydrophobic molecules like hexane, as seen in Figure 5c. At higher RH in the range of 50%−67%, the DNA becomes hydrated and vapors may displace weakly held water, yielding an enhanced response. At the highest RH levels approaching 100%, sensitivity appears to decrease significantly. The decrease is most likely caused by an increasing ionic conduction contribution that is insensitive to vapor sorption. Representative effects of RH levels on sensor response for a range of analyte concentrations are shown in Figure 6. The data reflect similar trends as Figure 5. Under dry conditions sensors respond linearly with resistance changes proportional to concentration and resemble swelling-dominated alkanethiol−AuNP chemiresistive sensors.[1,2,50] At higher RH values, resistance decreases proportional to concentration, except at 17, 84, and 99% RH where the responses is muted.

A decrease of resistance upon vapor sorption has also been reported for TOABr/AuNP mixtures with both polar and nonpolar vapors.[2] It was speculated that solvation effects may increase ion mobility or cause restructuring of the AuNP film to enhance conductivity. Decreased resistance has also been observed in some alkanethiol-functionalized AuNP for sensing

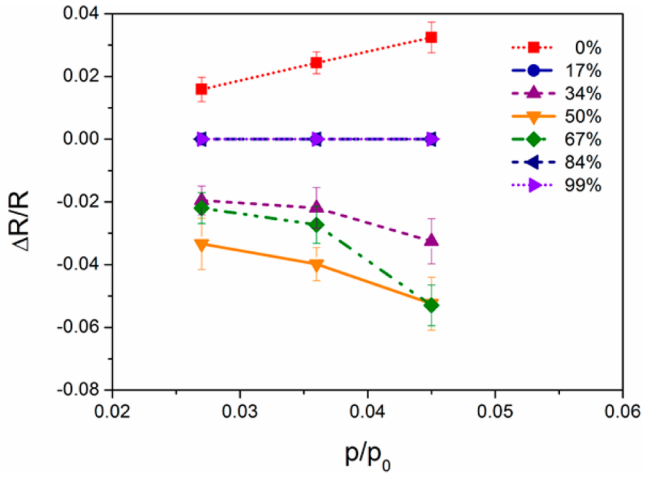

Figure 6. Effect of RH levels on responses toward ethanol at p/p_0 = 0.027, 0.036, and 0.045 on a set of poly C sensors.

of polar molecules such as water and alcohols.[1,50] Water vapor, in particular, could enhance ionic conductivity from impurities in films.[49] An explanation for the negative $\Delta R/R$ regions observed here is possibly more complicated since in addition to previously offered explanations there is the possibility of ligand-binding induced release of water from the hydration shell around the DNA.

SUMMARY AND CONCLUSIONS

In summary, we have fabricated chemiresistive vapor sensors using DNA-functionalized AuNPs. In contrast to most alkanethiol-functionalized AuNPs, DNA-functionalized gold nanoparticle sensors are highly sensitive to water sorption. At low relative humidity (up to 40%), sensors behave similarly to organothiol-functionalized gold nanoparticle sensors that respond to vapor partitioning and film swelling. At higher humidity (40%−100%), sensors behave increasingly like a polyelectrolyte with ionic conduction contributions to the electrical response. The high sensitivity to humidity indicates that careful control of water content is needed to distinguish analytes. The sensing of five vapors with four ss-DNA oligomer sequences was studied at different relative humidity values, and sequence-dependent response patterns were observed. The findings suggest that DNA-functionalized gold nanoparticle chemiresistors are comparable to alkanethiol−AuNP chemiresistive vapor sensors in terms of sensitivity and LOD. While cost and complexity likely do not justify the use of random DNA as a weakly specific sensing material, understanding effects such as base sequence and sensing conditions will be necessary to design improved sensors that use aptamers for high specificity. Continued study is needed to build the foundation for high specificity vapor sensing with DNA materials.

AUTHOR INFORMATION

Corresponding Author

*E-mail bgwillis@engr.uconn.edu (B.G.W.).

Notes

The authors declare no competing financial interest.

ACKNOWLEDGMENTS

The research is supported by Office of Naval Research Grant No. N00014-12-1-0088 and NSF Grant No. 1322332. K.F.

thanks Han Wang, Nathanael Chan, Andrew LaMarche, Wyatt Pedrick, and Yumin Zhu for assistance in preparing this manuscript.

REFERENCES

(1) Wohltjen, H.; Snow, A. W. Colloidal Metal–Insulator–Metal Ensemble Chemiresistor Sensor. *Anal. Chem.* **1998**, *70* (14), 2856–2859.
(2) Ibañez, F. J.; Zamborini, F. P. Chemiresistive Sensing of Volatile Organic Compounds with Films of Surfactant-Stabilized Gold and Gold–Silver Alloy Nanoparticles. *ACS Nano* **2008**, *2* (8), 1543–1552.
(3) Peng, G.; Tisch, U.; Adams, O.; Hakim, M.; Shehada, N.; Broza, Y. Y.; Billan, S.; Abdah-Bortnyak, R.; Kuten, A.; Haick, H. Diagnosing Lung Cancer in Exhaled Breath Using Gold Nanoparticles. *Nat. Nanotechnol.* **2009**, *4* (10), 669–673.
(4) Joseph, Y.; Guse, B.; Vossmeyer, T.; Yasuda, A. Gold Nanoparticle/Organic Networks as Chemiresistor Coatings: The Effect of Film Morphology on Vapor Sensitivity. *J. Phys. Chem. C* **2008**, *112* (32), 12507–12514.
(5) Fan, Z.; Wang, D.; Chang, P.-C.; Tseng, W.-Y.; Lu, J. G. ZnO Nanowire Field-Effect Transistor and Oxygen Sensing Property. *Appl. Phys. Lett.* **2004**, *85* (24), 5923–5925.
(6) Kauffman, D. R.; Star, A. Carbon Nanotube Gas and Vapor Sensors. *Angew. Chem., Int. Ed.* **2008**, *47* (35), 6550–6570.
(7) He, C.; Zhu, D.; He, Q.; Shi, L.; Fu, Y.; Wen, D.; Cao, H.; Cheng, J. A Highly Efficient Fluorescent Sensor of Explosive Peroxide Vapor via ZnO Nanorod Array Catalyzed Deboronation of Pyrenyl Borate. *Chem. Commun.* **2012**, *48* (46), 5739–5741.
(8) Wohltjen, H. Mechanism of Operation and Design Considerations for Surface Acoustic Wave Device Vapour Sensors. *Sens. Actuators* **1984**, *5* (4), 307–325.
(9) Barnard, S. M.; Walt, D. R. Fiber-Optic Organic Vapor Sensor. *Environ. Sci. Technol.* **1991**, *25* (7), 1301–1304.
(10) Tamane, S.; Topal, C. O.; Kalkan, A. K. In Vapor phase SERS sensor for explosives detection; Nanotechnology (IEEE-NANO), 2011 11th IEEE Conference on 15–18 Aug 2011; pp 301–306.
(11) Han, L.; Shi, X.; Wu, W.; Kirk, F. L.; Luo, J.; Wang, L.; Mott, D.; Cousineau, L.; Lim, S. I. I.; Lu, S.; Zhong, C.-J. Nanoparticle-Structured Sensing Array Materials and Pattern Recognition for VOC Detection. *Sens. Actuators, B* **2005**, *106* (1), 431–441.
(12) Lee, J.-O.; So, H.-M.; Jeon, E.-K.; Chang, H.; Won, K.; Kim, Y. Aptamers as Molecular Recognition Elements for Electrical Nanobiosensors. *Anal. Bioanal. Chem.* **2008**, *390* (4), 1023–1032.
(13) Ehrentreich-Förster, E.; Orgel, D.; Krause-Griep, A.; Cech, B.; Erdmann, V.; Bier, F.; Scheller, F. W.; Rimmele, M. Biosensor-Based on-Site Explosives Detection Using Aptamers as Recognition Elements. *Anal. Bioanal. Chem.* **2008**, *391* (5), 1793–1800.
(14) White, J.; Truesdell, K.; Williams, L. B.; AtKisson, M. S.; Kauer, J. S. Solid-State, Dye-Labeled DNA Detects Volatile Compounds in the Vapor Phase. *PLoS Biol.* **2008**, *6* (1), e9.
(15) Samain, F.; Ghosh, S.; Teo, Y. N.; Kool, E. T. Polyfluorophores on a DNA Backbone: Sensors of Small Molecules in the Vapor Phase. *Angew. Chem., Int. Ed.* **2010**, *49* (39), 7025–7029.
(16) Staii, C.; Johnson, A. T.; Chen, M.; Gelperin, A. DNA-Decorated Carbon Nanotubes for Chemical Sensing. *Nano Lett.* **2005**, *5* (9), 1774–1778.
(17) Kybert, N. J.; Lerner, M. B.; Yodh, J. S.; Preti, G.; Johnson, A. T. C. Differentiation of Complex Vapor Mixtures Using Versatile DNA–Carbon Nanotube Chemical Sensor Arrays. *ACS Nano* **2013**, *7* (3), 2800–2807.
(18) Lu, Y.; Goldsmith, B. R.; Kybert, N. J.; Johnson, A. T. C. DNA-Decorated Graphene Chemical Sensors. *Appl. Phys. Lett.* **2010**, *97* (8), 083107.
(19) Hammock, M. L.; Knopfmacher, O.; Naab, B. D.; Tok, J. B.-H.; Bao, Z. Investigation of Protein Detection Parameters Using Nanofunctionalized Organic Field-Effect Transistors. *ACS Nano* **2013**, *7* (5), 3970.
(20) Fuller, W.; Forsyth, T.; Mahendrasingam, A. Water–DNA Interactions As Studied by X-ray and Neutron Fibre Diffraction. *Philos. Trans. R. Soc., B* **2004**, *359* (1448), 1237–1248.
(21) Hanczyc, P.; Åkerman, B.; Nordén, B. Short Oligonucleotides Aligned in Stretched Humid Matrix: Secondary DNA Structure in Poly(vinyl alcohol) Environment. *Langmuir* **2012**, *28* (16), 6662–6669.
(22) Zilberman, Y.; Ionescu, R.; Feng, X.; Müllen, K.; Haick, H. Nanoarray of Polycyclic Aromatic Hydrocarbons and Carbon Nanotubes for Accurate and Predictive Detection in Real-World Environmental Humidity. *ACS Nano* **2011**, *5* (8), 6743–6753.
(23) Bayn, A.; Feng, X.; Müllen, K.; Haick, H. Field Effect Transistors Based on Polycyclic Aromatic Hydrocarbons for the Detection and Classification of Volatile Organic Compounds. *ACS Appl. Mater. Interfaces* **2013**, *5* (8), 3431–3440.
(24) Zellers, E. T.; Han, M. Effects of Temperature and Humidity on the Performance of Polymer-Coated Surface Acoustic Wave Vapor Sensor Arrays. *Anal. Chem.* **1996**, *68* (14), 2409–2418.
(25) Falk, M.; Poole, A. G.; Goymour, C. G. Infrared Study of the State of Water in the Hydration Shell of DNA. *Can. J. Chem.* **1970**, *48* (10), 1536–1542.
(26) Tao, N. J.; Lindsay, S. M. Structure of DNA Hydration Shells Studied by Raman-Spectroscopy. *Biopolymers* **1989**, *28* (5), 1019–1030.
(27) Liu, J.; Lu, Y. Preparation of Aptamer-Linked Gold Nanoparticle Purple Aggregates for Colorimetric Sensing of Analytes. *Nat. Protocols* **2006**, *1* (1), 246–252.
(28) Demers, L. M.; Mirkin, C. A.; Mucic, R. C.; Reynolds, R. A.; Letsinger, R. L.; Elghanian, R.; Viswanadham, G. A Fluorescence-Based Method for Determining the Surface Coverage and Hybridization Efficiency of Thiol-Capped Oligonucleotides Bound to Gold Thin Films and Nanoparticles. *Anal. Chem.* **2000**, *72* (22), 5535–5541.
(29) Pomogailo, A. D.; Kestelman, V. N. Principles and Mechanisms of Nanoparticle Stabilization by Polymers. In *Metallopolymer Nanocomposites*; Springer: Berlin, 2005; Vol. *81*, pp 65–113.
(30) Storhoff, J. J.; Elghanian, R.; Mirkin, C. A.; Letsinger, R. L. Sequence-Dependent Stability of DNA-Modified Gold Nanoparticles. *Langmuir* **2002**, *18* (17), 6666–6670.
(31) Herne, T. M.; Tarlov, M. J. Characterization of DNA Probes Immobilized on Gold Surfaces. *J. Am. Chem. Soc.* **1997**, *119* (38), 8916–8920.
(32) Petrovykh, D. Y.; Kimura-Suda, H.; Whitman, L. J.; Tarlov, M. J. Quantitative Analysis and Characterization of DNA Immobilized on Gold. *J. Am. Chem. Soc.* **2003**, *125* (17), 5219–5226.
(33) Petrovykh, D. Y.; Kimura-Suda, H.; Tarlov, M. J.; Whitman, L. J. Quantitative Characterization of DNA Films by X-ray Photoelectron Spectroscopy. *Langmuir* **2004**, *20* (2), 429–440.
(34) Ray, S. G.; Cohen, H.; Naaman, R.; Rabin, Y. Where Is the Sodium in Self-Assembled Monolayers of Single-Stranded DNA? *J. Am. Chem. Soc.* **2005**, *127* (49), 17138–17139.
(35) Mourougou-Candoni, N.; Naud, C.; Thibaudau, F. Adsorption of Thiolated Oligonucleotides on Gold Surfaces: An Atomic Force Microscopy Study. *Langmuir* **2003**, *19* (3), 682–686.
(36) Levicky, R.; Herne, T. M.; Tarlov, M. J.; Satija, S. K. Using Self-Assembly to Control the Structure of DNA Monolayers on Gold: A Neutron Reflectivity Study. *J. Am. Chem. Soc.* **1998**, *120* (38), 9787–9792.
(37) Zhang, R. Y.; Pang, D. W.; Zhang, Z. L.; Yan, J. W.; Yao, J. L.; Tian, Z. Q.; Mao, B. W.; Sun, S. G. Investigation of Ordered ds-DNA Monolayers on Gold Electrodes. *J. Phys. Chem. B* **2002**, *106* (43), 11233–11239.
(38) Joseph, Y.; Guse, B.; Yasuda, A.; Vossmeyer, T. Chemiresistor Coatings from Pt- and Au-Nanoparticle/Nonanedithiol Films: Sensitivity to Gases and Solvent Vapors. *Sens. Actuators, B* **2004**, *98* (2–3), 188–195.
(39) Han Ha, D.; Nham, H.; Yoo, K.-H.; So, H.-m.; Lee, H.-Y.; Kawai, T. Humidity Effects on the Conductance of the Assembly of DNA Molecules. *Chem. Phys. Lett.* **2002**, *355* (5–6), 405–409.

(40) Pang, P.; Guo, Z.; Cai, Q. Humidity Effect on the Monolayer-Protected Gold Nanoparticles Coated Chemiresistor Sensor for VOCs Analysis. *Talanta* **2005**, *65* (5), 1343−1348.
(41) Segev-Bar, M.; Shuster, G.; Haick, H. Effect of Perforation on the Sensing Properties of Monolayer-Capped Metallic Nanoparticle Films. *J. Phys. Chem. C* **2012**, *116* (29), 15361−15368.
(42) Chalikian, T. V.; Sarvazyan, A. P.; Plum, G. E.; Breslauer, K. J. Influence of Base Composition, Base Sequence, and Duplex Structure on DNA Hydration - Apparent Molar Volumes and Apparent Molar Adiabatic Compressibilities of Synthetic and Natural DNA Duplexes at 25 °C. *Biochemistry* **1994**, *33* (9), 2394−2401.
(43) Berman, H. M.; Sowri, A.; Ginell, S.; Beveridge, D. A Systematic Study of Patterns of Hydration in Nucleic-Acids. 1. Guanine and Cytosine. *J. Biomol. Struct. Dyn.* **1988**, *5* (5), 1101−1110.
(44) Zhou, Y.; Qin, Z.-Y.; Li, L.; Zhang, Y.; Wei, Y.-L.; Wang, L.-F.; Zhu, M.-F. Polyaniline/Multi-walled Carbon Nanotube Composites with Core−Shell Structures As Supercapacitor Electrode Materials. *Electrochim. Acta* **2010**, *55* (12), 3904−3908.
(45) Mao, L.; Zhang, K.; On Chan, H. S.; Wu, J. Surfactant-Stabilized Graphene/Polyaniline Nanofiber Composites for High Performance Supercapacitor Electrode. *J. Mater. Chem.* **2012**, *22* (1), 80−85.
(46) Ibañez, F. J.; Zamborini, F. P. Chemiresistive Sensing with Chemically Modified Metal and Alloy Nanoparticles. *Small* **2012**, *8* (2), 174−202.
(47) Note: the data for ethanol in Figure 5a are slightly different than in Figure 4b because data from Figure 5a are from different devices. Qualitatively, the responses are similar.
(48) Steinecker, W. H.; Rowe, M. P.; Zellers, E. T. Model of Vapor-Induced Resistivity Changes in Gold−Thiolate Monolayer-Protected Nanoparticle Sensor Films. *Anal. Chem.* **2007**, *79* (13), 4977−4986.
(49) Guo, J. L.; Pang, P. F.; Cai, Q. Y. Effect of Trace Residual Ionic Impurities on the Response of Chemiresistor Sensors with Dithiol-Linked Monolayer-Protected Gold (Nano)clusters as Sensing Interfaces. *Sens. Actuators, B* **2007**, *120* (2), 521−528.
(50) Han, L.; Daniel, D. R.; Maye, M. M.; Zhong, C. J. Core-Shell Nanostructured Nanoparticle Films As Chemically Sensitive Interfaces. *Anal. Chem.* **2001**, *73* (18), 4441−4449.

■ NOTE ADDED AFTER ASAP PUBLICATION

This paper was published on the Web on October 31, 2013, with an omission in the Figure 4 caption. The corrected version was reposted on November 4, 2013.